ACS APPLIED MATERIALS & INTERFACES

RESEARCH ARTICLE

www.acsami.org

Thermal Expansion and Contraction of an Elastomer Stamp Causes Position-Dependent Polymer Patterns in Capillary Force Lithography

Bongsoo Kim,[†] Minwoo Park,[†] Youn Sang Kim,[‡,§] and Unyong Jeong*,[†]

[†]Department of Materials Science and Engineering, Yonsei University, 134 Shinchon-dong, Seoul 120-749, Korea

[‡]Department of Nano Science and Technology, Graduate School of Convergence Science and Technology, Seoul National University, Gwanak-ro 1, Gwanak-gu, Seoul, 151-742, Korea

[§]Advanced Institute of Convergence Technology, Seoul National University, 864-1, Iui-dong, Yeongtong-gu, Suwon-si, Gyeonggi-do, Korea

S Supporting Information

ABSTRACT: It is often observed that polymer patterns fabricated by capillary force lithography (CFL) are not identical, position-dependent even in one sample. The drawback has not been successfully explained so far. This paper reveals that the position-dependent pattern is mainly caused by the volume expansion and contraction of the elastomer stamp during heating and cooling in the CFL process. The stamp expands on a polymer liquid on heating, accumulating the polymer at one side-wall of each pattern of the stamp. And the stamp shrinks back to the initial position, accumulating the polymer at the opposite wall of the stamp pattern. For crystalline polymers, the morphology was mainly determined by the annealing temperature, that is, the degree of expansion. The position-dependence of the morphology was enhanced as the annealing temperature was increased. For amorphous polymers, the morphology was sensitive to cooling rate. Fast cooling led to a frozen morphology generated at the hot annealing temperature, while slow cooling produced an opposite morphology from the one at the annealing. The experimental results were theoretically explained by analyzing thermal expansion of the stamp and the shear stress exerted in the polymer layer. In the conclusion, we added our suggestions to avoid the nonuniformity in the polymer pattern by CFL process.

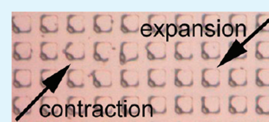

KEYWORDS: capillary force lithography, soft lithography, thermal expansion, elastomer stamp, polymer pattern, polymer thin film

1. INTRODUCTION

Soft lithography has received a lot of attention for micro- and nanofabrication because it is readily applicable to the current printing technology and biological area.[1,2] Soft lithography is based on an elastomer stamp that is typically poly(dimethylsiloxane) (PDMS), including microcontact printing (μCP),[3,4] nanoimprint lithography (NIL),[5,6] micromolding in capillaries (MIMIC),[7] and capillary force lithography (CFL).[8,9] Among the unconventional lithography techniques, CFL is the simplest and shows a reliable fidelity of pattern transfer.[10] The process only requests placing an elastomer stamp on a polymer thin film and raising the temperature above the glass transition temperature (T_g) or the melting temperature (T_m) of the polymer layer, and then cooling down to room temperature. A variety of complex patterns can be created by adjusting the annealing temperature and the thickness of polymeric layers on substrates.[11] A second stamping in a different angle can diversify the patterns accessible by CFL.[12]

Although CFL has been successful and widely employed to generate polymeric patterns, fine control of the patterned morphology has not been well achieved. Asymmetric line pattern has been often observed especially when the pattern of the stamp was large.[13] With a very thin polymer film, dual lines were generated at the corner of the stamp walls and the substrate, but the dimension of the lines was highly variant even in one sample.[14] In addition, the morphology was very different according to the position of the pattern in the stamp. A few groups tried to describe the experimental observations with thin film instability,[15,16] formation of meniscus at a stamp wall,[17] deformation of the stamp by mechanical pressure,[18] and interfacial energies between the polymer and the stamp as well as between the polymer and the substrate.[17] Unfortunately, the experimental observation of nonuniform asymmetric pattern could not be explained in a reasonable way by the analysis.

Here, we reveal that the position-dependent patterns are caused by thermal expansion and contraction of the elastomer stamp during annealing and cooling in the CFL process. We used the typical poly(dimethylsiloxane) (PDMS) stamps for the study. The PDMS stamps were made by mixing the base monomer and curing agent at 10:1 (w/w) (Sylgard 184, Dow corning). Because the stamp has a relatively large linear thermal expansion coefficient (3.0×10^{-4}/°C, obtained from the company Web site), it goes through considerable expansion and contraction on a polymer layer. Each pattern of the stamp travels forth and back by the thermal expansion and contraction, sweeping the polymer liquid. Because the travel distance of each pattern and the direction of the travel are dependent on the relative position from the center of the stamp, the resultant polymer pattern by CFL must be position-sensitive. In addition, we found that the annealing temperature and the cooling rate play important roles

Received: August 18, 2011
Accepted: October 10, 2011
Published: October 10, 2011

ACS Publications © 2011 American Chemical Society

in the morphology of the resultant polymer pattern. The morphological dependence on the position and the cooling rate could be theoretically explained.

2. EXPERIMENTAL SECTION

Materials. Poly(ε-caprolactone) (PCL, M_w = 42 500) was purchased from Aldrich. Poly(methyl methacrylate) (PMMA, M_n = 34 000, PDI = 1.05) was synthesized by anionic polymerization at −70 °C in degassed chloroform. The elastomer stamp was made of poly(dimethylsiloxane) (PDMS) by mixing the base monomer and curing agent at 10:1 (w/w) (Sylgard 184, Dow corning). The PDMS stamp was thermally cured at 80 °C for 1 day. A line-and-space stamp (10 μm feature size), a hexagonal-well stamp (20 μm side length), and a square-well stamp (10 μm side length) were made by casting on master patterns.

Capillary Force Lithography. PCL and PMMA solutions (3 wt %) in toluene were spin-coated at 3000 rpm for 30 s. The thickness of the thin films was 100 ± 7 nm measured by spectroscopic ellipsometer (SE MG-1000 Vis, Nanoview Co.). Highly concentrated polymer solutions (5, 6, 7 wt %) in toluene were used for thicker PCL films. A PDMS stamp was placed on a polymer thin film. The samples were annealed in a small heating chamber and then cooled down to room temperature. Development of polymer pattern and their morphological change was in situ monitored by an optical microscope (model BX 51, Olympus Co.). The final morphology after the CFL process was analyzed by an atomic force microscope (AFM, model dimension 3100, Digital Instrument Co.). For the samples with PCL, the heating temperature was raised up to 60 and 150 °C to control the extent of thermal expansion and contraction. The samples were in a heating block for 5 min and then cooled to room temperature. For the samples with PMMA, the heating temperature was fixed at 200 °C, but the cooling rate was controlled. After heating for 20 min at 200 °C, the samples were cooled down to 100 °C at a rate of −0.5, −10, or −20 °C/s. For fast quenching, the samples were placed on a cold metal plate.

3. RESULTS AND DISCUSSION

Because the PDMS stamp has a relatively large thermal expansion coefficient, the lateral movement of the PDMS stamp on a polymer liquid layer sweeps the polymer liquid forth on heating and back on cooling. The thermal expansion coefficient of the Si wafer is 2.6×10^{-6}/°C, which is ~100 times smaller than that of the PDMS stamp. Thermal expansion of the substrate was neglected in this study. The lateral movement (Δx) of a pattern at an initial position (x) from the center of the stamp can be determined by a following simple equation

$$\Delta x = \alpha(T - 25°\text{C})x \qquad (1)$$

, where α is a linear thermal expansion coefficient and T is an annealing temperature. The reference temperature is room temperature. The value of α was given from a company (Sylgard 184, $\alpha = 3.0 \times 10^{-4}$/°C). According to the equation, Δx is provided as a function of the position (x) in Figure 1. With a stamp having a 10 μm line-and-space pattern, Δx at x=2 mm from the center of the stamp was larger than the pattern period at any annealing temperature. For example, when annealed at 200 °C, the stamp pattern at x = 2 mm moved 105 μm which is 5 times longer than the pattern period of the stamp, while the pattern at x = 0.3 mm moved 16 μm which is less than the pattern period. The difference in the lateral movement of the pattern depending on the position leads to a position-dependent morphology with CFL.

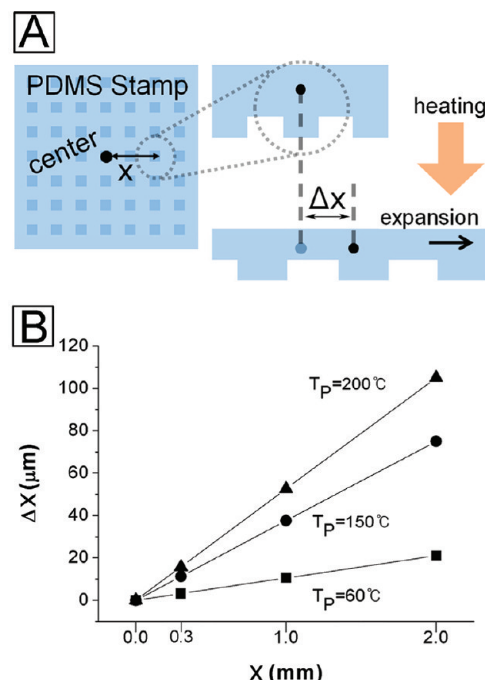

Figure 1. (A) Schematic illustration on the thermal expansion of the PDMS stamp. (B) Graphical representation of eq 1, showing the traveling distance (Δx) of the stamp according to the position (x) from the center of the stamp. Three annealing temperatures (T = 60, 150, 200 °C) were compared.

Although the morphological development during thermal annealing is thermodynamically determined, the extent of polymer sweeping during cooling should be sensitive to the viscosity of the polymer. Because a crystalline polymer is still very fluidic near its melting temperature (T_m), the polymer melt can flow even at a weak shear force so that the morphology generated at the annealing temperature can largely change even at a fast cooling rate. Therefore, the amount of thermal expansion and contraction that is determined by the annealing temperature is the governing factor to determine the morphology in a crystalline polymer. In contrast, chain mobility of an amorphous polymer considerably decreases even at a much higher temperature than its glass transition temperature (T_g).[17] Slow cooling gives enough time for the morphological change, but thermal quenching freezes the morphology generated at the annealing temperature. Therefore, cooling rate should be an important factor in an amorphous polymer. In this study, we investigated four representative cases: (i) a crystalline polymer at a low annealing temperature ($T \approx T_m$), (ii) a crystalline polymer at a high annealing temperature ($T \gg T_m$), (iii) an amorphous polymer at a slow cooling rate, and (iv) an amorphous polymer at a fast cooling rate. PCL and PMMA were chosen as the crystalline and amorphous polymers.

Figure 2 is a schematic illustration for the morphological change of a crystalline polymer layer during the heating and cooling process. When $T < T_{m,polymer}$, the stamp cannot expand due to the large friction between the stamp and a solid polymer. When the annealing temperature reaches T_m ($T \approx T_m$), the polymer thin film starts to dewet and rises on the PDMS wall by the capillary force. Capillary rise is driven by the tendency to keep the contact angle between the stamp and the polymers. The hydrophobic polymers, PCL and PMMA in this study, have

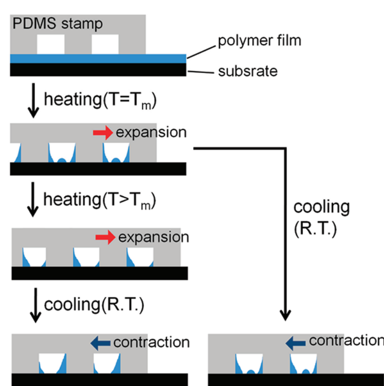

Figure 2. Schematic illustration on the morphological development of a crystalline polymer by the thermal expansion and contraction of a PDMS stamp. Above the melting temperature (T_m) of the polymer, the polymer liquid rises up on the PDMS walls by the capillary force. Thermal expansion (moving to the right) accumulates the polymer at the left-side wall of each stamp pattern and volume contraction (moving to the left) does at the opposite wall. The final morphology depends on the annealing temperature, that is, the extent of thermal expansion and contraction.

better affinity to the PDMS stamp than to the hydrophilic Si surface. In addition to the capillary rise, the stamp expands in the radial direction and each stamp pattern sweeps the polymer liquids. Small amount of polymer melt is accumulated at one side of the PDMS wall (left wall in Figure 2) during heating. Cooling down to room temperature from the low annealing temperature makes the stamp sweep the polymer liquid in the reverse direction so that the polymer melt can be evenly distributed at both PDMS walls. Small polymer droplets can be made in the middle due to the dewetting of the polymer liquid on the Si wafer surface. Thin film instability is determined by combination between the long-range interaction and the short-range interaction. Most polymer liquids dewet via the binodal instability or via a combination of the spinodal and binodal instabilities unless the polymers and the substrate have a strong van der Waals attraction.

When the annealing temperature is high ($T \gg T_m$), the stamp expands a lot and the patterns sweep the polymer melt to a long distance so that large amount of the polymer is accumulated at the left-wall of the pattern. On cooling to room temperature, the PDMS stamp retracts until the temperature becomes lower than T_m of the polymer. This reverse movement, in turn, accumulates a large portion of the polymer at the opposite wall of the stamp pattern (right wall in Figure 2), which produces an asymmetric morphology. Although we described the scheme with a temperature change, actual effect comes from the travel distance of the stamp pattern during heating and cooling. The travel distance increases with the distance (x) from the center of the stamp as seen in Figure 1. Thereby, the morphology must be different even in one sample according to the distance (x) from the center. Another important factor determining the morphology is the direction of expansion and contraction of a stamp pattern from the center of the stamp. In addition, the pattern shape of the stamp plays a critical role on the final morphology.

Figure 3 shows an experimental result from the crystalline polymer (PCL) processed at a low annealing temperature (60 °C, $T = T_m$). Thickness of the PCL film was 96 nm. A PDMS stamp with large hexagonal-well patterns (20 μm length of side wall) was employed. The optical microscope (OM) images in Figure 3A obviously visualize the difference in accumulation of

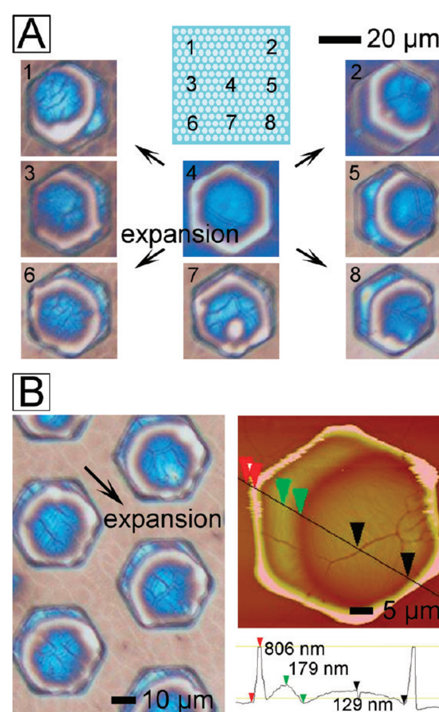

Figure 3. (A) Optical microscope image from a crytstalline polymer, poly(ε-carprolactone) (PCL), at a low annealing temperature ($T = T_m$, 60 °C). The numbers indicate the relative position from the center of the stamp. No. 3 and 5 were 0.3 mm away from the center ($x = 0.3$ mm), which led to small traveling distance ($\Delta x \approx 3$ μm) compared to the feature (20 μm side length) of the hexagonal-well pattern. According to x and the expansion direction, the asymmetric morphology was varied. (B) Atomic force microscope (AFM) image of (8).

the polymer melt in each stamp pattern, depending on the relative position from the center of the stamp and the relative direction to the thermal expansion. Eight positions in the stamp are marked with numbers. Colored parts indicate thicker polymer layers. The hexagonal well at the center of stamp 4 had isotropic volume expansion in every radial direction so that there was no net lateral movement of the stamp well. At this position, PCL evenly rose up on the wall of the well and the residual PCL formed a large droplet in the middle of the well as seen in blue. At positions away from the center of the stamp, lateral movement of the well by expansion made the polymer accumulated on one side wall of the well. The accumulated polymer during annealing was swept back during cooling, now being accumulated at the other wall of the stamp pattern. Figure 3B represents the height profile in one pattern at position 8, which is 0.3 mm apart from the center. The value of Δx was 3.15 μm, which is smaller than the pattern period. The rising of the polymer on the PDMS wall was seen at both side-walls. However, large portion of PCL was accumulated at one side-wall of the pattern and a large droplet is placed closer to the opposite wall.

When the annealing temperature was much higher than the melting temperature ($T \gg T_{m,polymer}$), the large thermal expansion led to net lateral movement of the stamp pattern longer than the pattern period. The results in Figure 4 were obtained by annealing at 150 °C with a line-and-space stamp (10 μm feature size) on a 96 nm thick PCL film. AFM images in Figure 4A exhibit three different positions (the center of the stamp, left from the center, and right from the center. The right and left

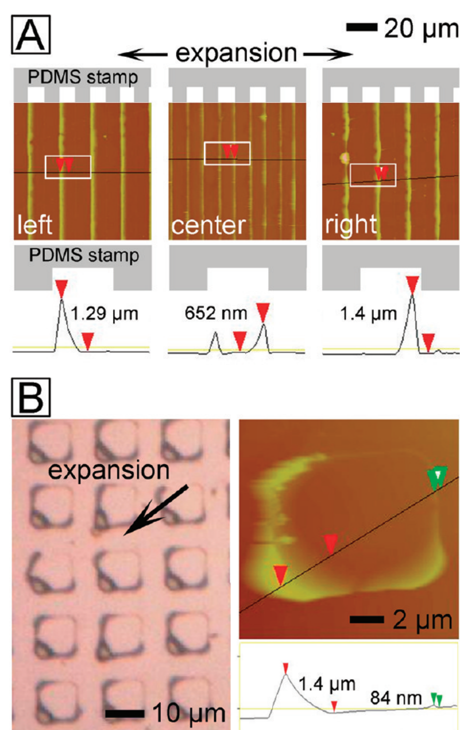

Figure 4. Asymmetric morphology of PCL obtained by heating at a high temperature (150 °C, $x = 2$ mm, $\Delta x = 75$ μm). (A) AFM images by a line-and-space pattern stamp. At the center of the stamp, the polymer distribution was symmetric. The polymer was selectively accumulated at the left-side wall of the PDMS patterns in the left position from the stamp center. The opposite was observed in the right position. (B) AFM and OM images by a square-well stamp. The stamp patterns were located left and bottom from the center of the stamp. The polymer was accumulated at the bottom corner.

positions were 2 mm apart from the center ($x = 2$ mm). We did not observe the residual polymer droplet on the substrate with this pattern size. In the pattern at the center of the stamp, there was no net lateral movement of the pattern so that PCL was evenly distributed at both walls, thereby symmetric dual lines were obtained. In the left position, the net movement of the pattern was about 80 μm that was longer than the pattern size. The polymer was swept by the right-side wall of the pattern during the expansion and swept reverse by the left-side wall during the contraction. Resultantly, PCL was accumulated more at the left-side wall in the final morphology. The polymer in the right position from the center of the stamp experienced the same event, but in the opposite direction, leading to more accumulation at the right-side wall of the pattern. The similar results could be observed in a PDMS stamp with square wells. The OM image in Figure 4B displays a highly asymmetric distribution of PCL in square wells. The stamp pattern was located left and down from the center of the stamp, so the movement of the patterns was diagonal for the square. The asymmetric accumulation of PCL at a bottom corner was due to the sweeping of the polymer during the cooling process. Use of a PDMS stamp with a high modulus can decrease its thermal expansion, but it can disturb the conformal contact of the stamp on the surface and generate many defects in the polymer pattern. We tested high modulus stamps as long as they can produce reproducible polymer patterns. Unfortunately, position-dependence of the pattern was inevitable.

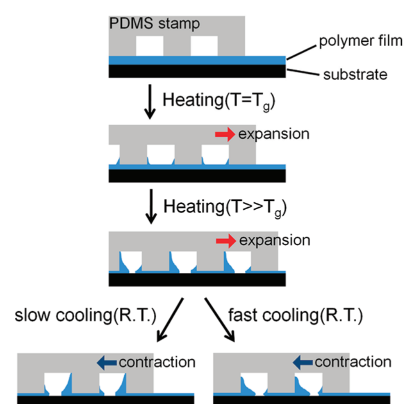

Figure 5. Schematic illustration on the morphological development of an amorphous polymer by the thermal expansion and contraction of a PDMS stamp. Above the glass transition temperature (T_g) of the polymer, the polymer liquid rises up on the PDMS walls by the capillary force. Thermal expansion (moving right) accumulates the polymer at the left-side wall and contraction (moving left) does at the opposite wall. The final morphology depends on the cooling rate.

The high chain mobility of the crystalline melt even near the melting temperature allowed their fast sweeping by the stamp pattern during the cooling process so that kinetic effect of the chain relaxation was not considerable in the overall morphology. In contrast, viscosity of an amorphous polymer rapidly increases as the temperature approaches its glass transition temperature (T_g), so liquid flow is greatly hindered even at temperatures much higher than T_g of the polymer. Because the relative distribution of the polymer in each pattern must depend on the sweeping degree of the polymer melt during the cooling process, the final morphology by CFL on an amorphous polymer can be varied by adjusting the cooling rate. The scheme in Figure 5 describes asymmetric accumulation of an amorphous polymer according to a slow and a fast cooling rate. The high viscosity of amorphous polymers leaves a residual layer under the stamp. The PDMS stamp cannot laterally expand before the heating temperature reaches T_g of the polymer due to the friction between the stamp and the polymer thin film. At T_g, the stamp starts to expand and the polymer melt rises on the stamp wall. As the annealing temperature increases, the stamp sweeps the polymer melt and more polymer melt is collected on the left-side wall of the stamp pattern as seen in Figure 5. On cooling, the stamp starts to sweep the polymer in the reverse direction. With slow cooling rate, the polymer melt can be accumulated on the right-side wall in Figure 5. Meanwhile, fast cooling does not give enough time for the polymer chains to relax so that the final pattern should be similar to the morphology at the annealing temperature.

Quantitative analysis on the morphology from an amorphous polymer requests the information of the shear stress at the PDMS-polymer interface ($\sigma_{\text{PDMS-polymer}}$) during the cooling process. $\sigma_{\text{PDMS-polymer}}$ is the same with the contraction force of the PDMS stamp exerted on the interface. We suppose that $\sigma_{\text{PDMS-polymer}}$ should be higher than a critical shear stress (σ_{critical}) at which the polymer layer can flow. The maximum contraction force ($F_{\text{PDMS},T}$) from a certain annealing temperature can be obtained from the thermal expansion coefficient as following

$$\mathrm{F}_{\text{PDMS},\,T} = A_c\sigma_{\text{PDMS}} = (h \times l)E_{\text{PDMS}}\alpha\Delta T \qquad (2)$$

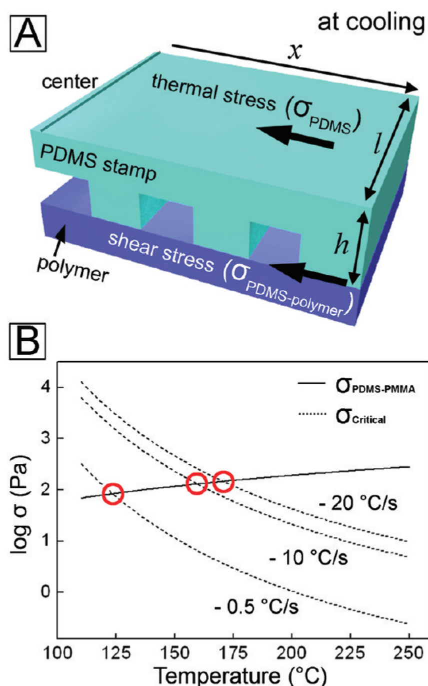

Figure 6. (A) Schematic illustration including the shear stress ($\sigma_{\text{PDMS-polymer}}$) exerted on a polymer by the contraction of the stamp. (B) Analysis on the shear stress for an amorphous polymer, poly(methylmethacrylate) (PMMA). The critical shear stress (σ_{critical}) is a shear stress at a certain strain rate which is linearly proportional to the cooling rate. Depending on the cooling rate, the morphology is frozen at the temperatures below the cross sections (indicated by red circles) between $\sigma_{\text{PDMS-polymer}}$ and σ_{critical}.

where A_c, h, and l are the cross-sectional area, the thickness, and the width of the PDMS stamp, as depicted in Figure 6A. The reference for ΔT is room temperature ($\Delta T = T - 25°\text{C}$). Young's modulus of PDMS (E_{PDMS}) has linear relation with ΔT.

$$E_{\text{PDMS},T} = E_{\text{PDMS},25°\text{C}} + b\Delta T \tag{3}$$

The value of $E_{\text{PDMS},25°\text{C}}$ was 1.75 MPa.[19] The coefficient (b) is quoted from a literature,[19] $b = (3)/(2)k\rho_k$, where k is Boltzmann constant and ρ_k is the cross-linking density of the PDMS ($\rho_k = 4.93 \times 10^{26}$ m^{-3}) for the 10:1 condition. The maximum shear stress on the polymer layer ($\sigma_{PDMS\text{-polymer}}$) by the cooling from the annealing temperature (T) can be obtained.

$$\sigma_{\text{PDMS-polymer}}(T) = \frac{F_{\text{PDMS},T}}{A_i} = \frac{F_{\text{PDMS},T}}{c(xl)}$$
$$= \frac{h}{cx}\alpha\Delta T(E_{\text{PDMS},25°\text{C}} + b\Delta T) \tag{4}$$

where c is the fraction of the contact area (A_i) in the whole stamp–polymer interface. An equally spaced line-and-space stamp has $c = 0.5$. For the critical shear stress of the polymer (σ_{critical}), we simplified the calculation by assuming a Newtonian fluid because the shear rate (here, the motion of the PDMS stamp) is not high. Therefore, we can get the equation like $\sigma_{\text{critical}}(T) = \eta_{0,T}\dot{\gamma}_T$ where $\eta_{0,T}$ is the zero-shear viscosity of the polymer at temperature T and $\dot{\gamma}_T$ is the shear strain rate. And $\eta_{0,T}$ can be calculated from the Williams–Landel–Ferry (WLF) equation ($\eta_{0,T} = \eta_{0,T_R}a_T$) with a proper choice of the shift factor (a_T, $\log a_T = -(C_1(T(T_R))/(C_2 + (T(T_R)))$. The shear strain rate can be expressed as the following

$$\dot{\gamma}_T = \frac{(\Delta x/d_{\text{polymer}})}{\Delta t} = \left(\frac{\alpha x\Delta T}{d_{\text{polymer}}\Delta t}\right) = \frac{\alpha x}{d_{\text{polymer}}}\dot{T} \tag{5}$$

where d_{PMMA} is the thickness of the polymer film and $\dot{T}$ is the cooling rate. Equation 5 expressed the strain rate of the polymer layer as a function of cooling rate. Via eq 5, $\sigma_{\text{critical}}(T)$ is derived.

$$\sigma_{\text{critical}}(T) = \eta_{0,T}\dot{\gamma}_T = \eta_{0,T_R}\frac{\alpha x}{d_{\text{polymer}}}a_T\dot{T} \tag{6}$$

Figure 6B is an example analysis with a PMMA (M_w = 34 000) as the polymer liquid. We used a monodisperse (PDI = 1.05) low-M_w PMMA synthesized by the anion polymerization. We wanted to remove time-dependency of the morphology formation often observed in CFL when a commercial PMMA with a high viscosity was used. The reference zero-shear viscosity (η_{0,T_R}) of the PMMA in this study was 3,434 Pa s at 200 °C which was calculated from the literature value (13 450 Pa s) of a PMMA (M_w = 100 000).[20] For the calculation, we employed the Fox and Flory equation ($\eta_0 = kM_w^{3.4}$). The literature values of the parameters for the shift factor were $C_1 = 7.67$ and $C_2 = 210.76$.[20] The thickness (d) of the PMMA layer was 100 nm. Figure 6B shows the changes in $\sigma_{\text{PDMS-PMMA}}$ and σ_{critical} according to the annealing temperature at the distance (x = 2 mm). The thickness of the PDMS stamp was set to be 1 mm for the calculation. Because the required shear stress is linearly proportional to the cooling rate (eq 6), we compared three different cooling rates, −0.5s, −10, and −20 °C/s. The cooling rate was controlled down to the glass transition temperature of PMMA (110 °C). $\sigma_{\text{PDMS-PMMA}}$ linearly increased with the annealing temperature, but σ_{critical} of the polymer was inversely proportional to the annealing temperature. When $\sigma_{\text{PDMS-PMMA}} < \sigma_{\text{critical}}$, the shear force is not considered large enough to induce polymer flow. Therefore, the polymer layer is not further deformed at that condition during the cooling process even though the PDMS stamp can still retract to the initial position. For example at a slow cooling rate of −0.5 °C/s, the polymer chains are frozen at ∼123 °C, which is close to the glass transition temperature. The final morphology will be considerably different from the one at the annealing temperature because the polymer melt can be swept long distance during the cooling process. In contrast, at a fast cooling rate of −20 °C/s, the deformation of the polymer layer stops at ∼172 °C. Therefore, if the annealing temperature is 180 °C, the overall morphology after cooling will be very similar to the morphology at the annealing temperature.

The modulus of a rubber is inversely proportional to the molecular weight between cross-linking sites, thereby it is proportional to the cross-linking density. However, it is noticeable that that the effect of cross-linking density in the thermal expansion is not considerable especially when the strain is small. Thermal expansion coefficients of the PDMS stamps with various modulus are added in the Supporting Information (Figure S1). We varied the composition of the PDMS monomer and the cross-linker to change the modulus. The modulus increased with the relative amount of cross-linker involved in the PDMS mixture (PDMS monomer: cross-linker, w/w), which was 0.08, 0.51, 1.751, 2.61, and 4.35 MPa at room temperature for 1:40, 1:20, 1:10, 1:5, and 1:2, in the order. We found no meaningful change in the thermal expansion of the stamps. Although the shear stress at the interface increases with the rubber modulus from eq 4, the

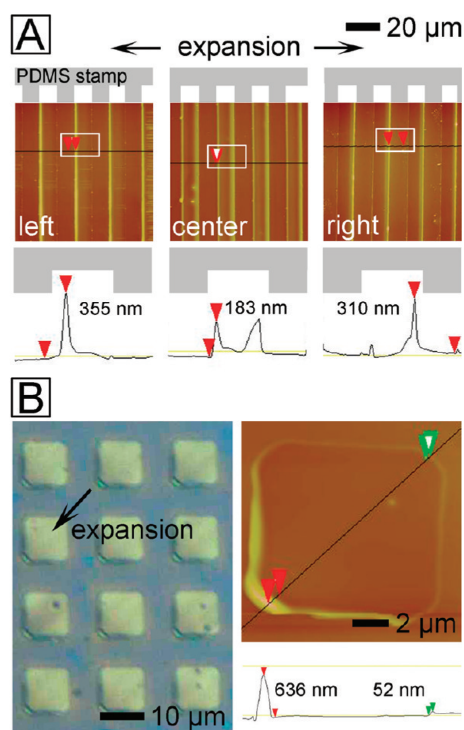

Figure 7. (A) Asymmetric morphology of PMMA obtained by a slow cooling (−0.5 °C/s) from a high annealing temperature (200 °C) at x = 2 mm and Δx = 105 μm. A line-and-space PDMS stamp (20 μm periodicity) was used. At the center of the stamp, the polymer was evenly distributed. The polymer was selectively accumulated at the left-side wall of the PDMS patterns in the left position from the stamp center. The opposite was observed in the right position. (B) AFM and OM images generated by a square-well stamp. The stamp patterns were located left and bottom from the center of the stamp.

modulus effect on the polymer pattern is not considerable because the dragging of the polymer melt is mainly driven by the moving distance, not by the elastic force.

Figure 7 shows experimental results obtained after CFL with a slow cooling on a 93 nm-thick PMMA thin film. The sample was annealed at 200 °C for 30 min in N_2 environment and cooled down at a rate of −0.5 °C/s. In Figure 7A, the stamp had a 10 μm feature size. The AFM images present the morphologies at three positions (center of the stamp, left and right that are 2 mm apart from the center (x = 2 mm)). In the pattern at the central position, overall distribution of PMMA was even. The morphology was the same with a longer annealing time, which tells 30 min annealing at 200 °C was enough for their morphological development in the pattern. Because the overall morphology is determined by the movement of the stamp, not by the capillary rise, the whole process reaches the final morphology within a few seconds. We found no difference in the morphology of the samples taken right after the movement of the stamp and taken after annealing for 30 min. It was the same for the crystalline polymers. The morphologies shown in this study represents the final states. The left and right position had lateral movement of the pattern by ∼105 μm, which was longer than the pattern period. At slow cooling, the patterns at the left position showed more accumulation of the polymer at the left-side wall and the patterns at the right position had the opposite accumulation, which is similar to the result with a crystalline polymer shown in Figure 5. The same phenomenon was observed in square-well patterns. Figure 7B shows the distribution of PMMA at a slow cooling with a square-well patterned PDMS stamp. The pattern was located at the left and down from the center of the stamp.

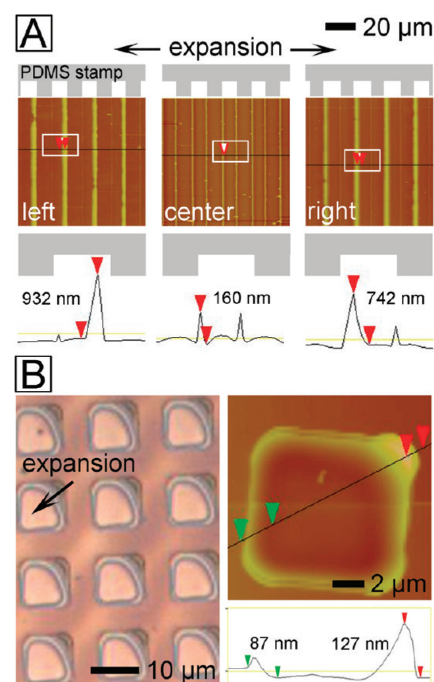

Figure 8. Asymmetric morphology of PMMA obtained by a fast cooling (−20 °C/s), but with the same conditions with Figure 7. Fast cooling led to opposite results to those obtained by a slow cooling.

Figure 8A displays the results by a fast cooling, but with the same other conditions. The sample was quickly removed from a small heating block and placed on a cold metal substrate. The central position showed an even polymer distribution at both walls, but the left and right position showed opposite results to those shown in Figure 7. It was because the morphology at 200 °C was frozen because of the fast solidification during cooling. It was the same in square-well patterns (Figure 8B).

The effect of thermal expansion and contraction of the stamp should depend on film thickness versus pattern dimension of the stamp. For a line-and-space pattern, the use of small feature-sized stamp on a thick film produced almost symmetric distribution of the polymer, while thin films with large feature-sized patterns showed the position-dependent asymmetric distribution of the polymer. Figure 9 displays the morphological dependence on the film thickness at a fixed stamp dimension. The AFM images were obtained with PCL thin films: (A) 180, (B) 300, and (C) 400 nm. The line-and-space pattern of the stamp had 5 μm feature size. The left and right position was 2 mm apart from the center of the stamp. In Figure 9A, PCL was accumulated at the left-side wall in the left position and at the right-side wall in the right position, which was similar to the results seen in Figure 4. When the film thickness was 300 nm, the CFL process generated single lines with a meniscus instead of distinct dual lines (Figure 9B). Suh et al. discussed that the critical volume of polymer in a pattern to form a meniscus can be calculated simply by the contact angle of the meniscus and dimension of the stamp.[15] We found the critical volume is not clear because the actual process involves the sweeping of the polymer in the pattern. At the single-line condition, the accumulated polymer melt by the expansion or contraction of the stamp can translate to the other side. Thereby,

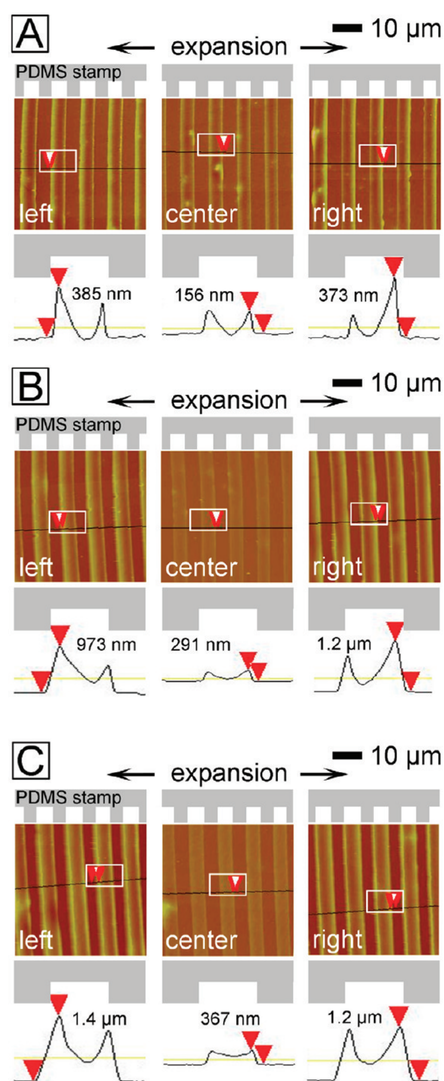

Figure 9. Morphological dependence on the film thickness at a fixed stamp dimension (line-and-space with a 10 μm periodicity). Thicknesses of the PCL film was (A) 180, (B) 300, and (C) 400 nm. The asymmetric pattern was not prominent as the thickness of the film increased.

the effect of thermal expansion and contraction was observed less as the thickness of the polymer film increased. Figure 9C demonstrates more symmetric distribution of PCL in the three positions, fabricated on a 400 nm film. It is noticeable that the thermal expansion effect was negligible when a low-viscosity polymer completely fills the channel of the stamp and cooling proceeds slowly. But, it remained a very thick residual layer, which is not desirable.

Because the thermal expansion depends on the position of the stamp pattern, Figure S2 in the Supporting Information shows an overall tendency of the polymer distribution in the stamp pattern. The heights of the polymer accumulation were measured by AFM. Figure S2A in the Supporting Information was obtained from a 96 nm-thick PCL layer and Figure S2B in the Supporting Information was taken from a 104 nm-thick PMMA layer by slow cooling. The line-and-space PDMS stamp had 5 μm feature size. As described in the inset images, the figures show the height at the right side of the stamp channel. The accumulation of the polymers on the right wall increased as the position was far from the center, meanwhile the accumulation on the left wall decreased, deteriorating the uniformity in accumulation. Compared to the right wall, the accumulation on the left wall showed a limited dependence, which is reasonable because the driving force to accumulate on the left wall is simply the capillary rise, not the stamp movement.

4. CONCLUSIONS

We demonstrated that the thermal expansion and contraction of the elastomer stamp is the reason of the position-dependent morphology which have been often observed in capillary force lithography (CFL). Because the elastomer stamp (PDMS in this study) has a relatively large thermal expansion coefficient, the stamp considerably expanded and contracted on heating and cooling. Each pattern of the stamp moved forth and back on a polymer liquid layer, accumulating the polymer at one side-wall on heating, and then at the opposite wall on cooling. For crystalline polymer melt, the accumulation in the cooling process resulted in the asymmetric morphology. The extent of the asymmetric accumulation was enhanced with the travel distance of each stamp pattern. This effect was prominent when the annealing temperature was much higher than T_m of the polymer. For amorphous polymers, slow cooling made a different morphology from the one at the annealing temperature, while fast cooling led to a frozen morphology at the annealing temperature. These experimental observations could be well-explained by a theoretical analysis involving the thermal expansion coefficient and shear stress on the film. The influence of the volume expansion and contraction was considerable in thin films, meanwhile it was not significant in thick films. If we want to avoid the nonuniformity of the polymer pattern by CFL process, there might be several possible ways: (i) minimizing the thermal expansion of the stamp by sticking a thin rubber stamp on a hard plate with a low thermal expansion coefficient, (ii) using a substrate with a similar thermal expansion coefficient with the rubber stamp, for example the same PDMS rubber substrate, (iii) treating the surface of the stamp to have a small adhesion with the polymer layer so that the stamp can slide on the polymer layer even when the polymer is a solid.

■ ASSOCIATED CONTENT

Supporting Information. Thermal expansion coefficient of the PDMS stamps having various moduli and position dependence of the pattern uniformity. This material is available free of charge via the Internet at http://pubs.acs.org/.

■ AUTHOR INFORMATION

Corresponding Author
*E-mail: ujeong@yonsei.ac.kr.

■ ACKNOWLEDGMENT

This research was supported by the National Research Foundation (NRF) grant funded by the Korean Government (MEST) through the Active Polymer Center Pattern Integration (R11-2007-050-01004-0), Basic Research Program (2011-0018113) and the World Class University (WCU) Program (R32-20031). B.K. thanks the Hi Seoul Science/Humanities Fellowship from Seoul Scholarship Foundation.

REFERENCES

(1) Geissler, M.; Xia, Y. *Adv. Mater.* **2004**, *16*, 1249–1269.
(2) Byun, M.; Han, W.; Li., B.; Hong, S. W.; Cho, J. W.; Zou, Q.; Lin, Z. *Small* **2011**, *7*, 1641–1646.
(3) Kumar, A.; Whitesides, G. M. *Appl. Phys. Lett.* **1993**, *63*, 2002–2004.
(4) Kumar, A.; Biebuyck, H. A.; Whitesides, G. M. *Langmuir* **1994**, *10*, 1498–1511.
(5) Guo, L. J. *Adv. Mater.* **2007**, *19*, 495–513.
(6) Chou, S. Y.; Krauss, P. R.; Renstrom, P. J. *J. Vac. Sci. Technol., B* **1996**, *14*, 4129–4133.
(7) Kim, E.; Xia, Y.; Whitesides, G. M. *J. Am. Chem. Soc.* **1996**, *118*, 5722–5731.
(8) Suh, K. Y.; Kim, Y. S.; Lee, H. H. *Adv. Mater.* **2001**, *13*, 1386–1389.
(9) Zhang, D.; Yu, W.; Wang, T.; Lu, Z.; Sun, Q. *Opt. Express* **2010**, *18*, 15009–15016.
(10) Bruinink, C. M.; Péter, M.; Maury, P. A.; de Boer, M.; Kuipers, L.; Huskens, J.; Reinhoudt, D. N. *Adv. Funct. Mater.* **2006**, *16*, 1555–1565.
(11) Kwak, R.; Jeong, H. E.; Suh, K. Y. *Small* **2009**, *5*, 790–794.
(12) Park, M.; Hyun, D. C.; Kim, J.; Kim, Y. S.; Jeong, J. *Chem. Mater.* **2010**, *22*, 4166–4174.
(13) Yoon, H.; Choi, M. K.; Suh, K. Y.; Char, K. *J. Colloid Interface Sci.* **2010**, *346*, 476–482.
(14) Suh, K. Y.; Lee, H. H. *J. Chem. Phys.* **2001**, *115*, 8204–8208.
(15) Park, J. Y.; Suh, K. Y.; Seo, S.; Lee, H. H. *J. Chem. Phys.* **2006**, *124*, 214710–214714.
(16) Suh, K. Y.; Yoo, P. J.; Lee, H. H. *Macromolecules* **2002**, *35*, 4414–4418.
(17) Bietsch, A.; Michel, B. *J. Appl. Phys.* **2000**, *88*, 4310–4318.
(18) Young, R. J.; Lovell, P. A. *Introduction to Polymers*, 2nd ed.; Chapman & Hall: London, 1991.
(19) Schneider, F.; Fellner, T.; Wilde, J.; Wallrabe, U. *J. Micromech. Microeng.* **2008**, *18*, 065008–065016.
(20) Aho, J.; Syrjälä, S. *Polym. Test* **2008**, *27*, 35–40.